Accelerated Publications

Correlation between Dynamics and High Affinity Binding in an SH2 Domain Interaction[†]

Lewis E. Kay,*[,‡] D. R. Muhandiram,[‡] Neil A. Farrow,[‡] Yves Aubin,[‡,§] and Julie D. Forman-Kay*[,§]

Protein Engineering Network Centres of Excellence and Departments of Medical Genetics, Biochemistry and Chemistry, University of Toronto, Toronto, Ontario, Canada M5S 1A8, and Biochemistry Research Division, Hospital for Sick Children, 555 University Avenue, Toronto, Ontario, Canada M5G 1X8

ABSTRACT: Protein−protein interfaces can consist of interactions between large numbers of residues of each molecule; some of these interactions are critical in determining binding affinity and conferring specificity, while others appear to play only a marginal role. Src-homology-2 (SH2) domains bind to proteins containing phosphorylated tyrosines, with additional specificity provided by interactions with residues C-terminal to the phosphotyrosine (pTyr) residue. While the C-terminal SH2 domain of phospholipase C-γ1 (PLCC SH2) interacts with eight residues of a pTyr-containing peptide from its high affinity binding site on the β-platelet-derived growth factor receptor, it can still bind tightly to a phosphopeptide containing only three residues. Novel deuterium (^{2}H) based nuclear magnetic resonance (NMR) spin relaxation experiments which probe the nanosecond−picosecond time scale dynamics of methyl containing side chain residues have established that certain regions of the PLCC SH2 domain contacting the residues C-terminal to the pTyr have a high degree of mobility in both the free and peptide complexed states. In contrast, there is significant restriction of motion in the pTyr binding site. These results suggest a correlation between the dynamic behavior of certain groups in the PLCC SH2 complex and their contribution to high affinity binding and binding specificity.

Protein-mediated recognition is a critical component in many biological processes, such as signal transduction. Protein−protein interfaces often show interactions between large numbers of residues across the interface. While some of these interactions are critical to recognition, others play only a marginal role in conferring significant binding energy and specificity (Clackson & Wells, 1995). In addition, many molecules involved in mediating protein recognition bind to multiple targets, with binding interfaces containing direct contacts to nonconserved residues [e.g., calmodulin (Klee & Vanaman, 1982; Vogel, 1994), troponin C (McCubbin &

Kay, 1980), and various proteins containing Src-homology-2 (SH2)[1] and Src-homology-3 domains (Pawson, 1995; Pawson & Schlessinger, 1993)]. It is not clear, however, what differentiates those regions of protein interfaces which contribute to binding and specific recognition from those that do not. Studies of the interaction of human growth hormone with the extracellular domain of its bound receptor failed to detect a correlation between the important residues in the "functional epitopes" of the interface and either buried

[1] Abbreviations: HSQC, heteronuclear single-quantum coherence; $J(\omega)$, power spectral density function; K_d, dissociation constant; NMR, nuclear magnetic resonance; NOE, nuclear Overhauser effect; PDGFR, platelet-derived growth factor receptor; PLC-γ1, phospholipase C-γ1; PLCC SH2, C-terminal SH2 domain of phospholipase C-γ1; ppm, parts per million; ps−ns, picosecond to nanosecond time scale; pTyr, phosphotyrosine; pY1021, the peptide DNDpYIIPLPDPK derived from the pTyr-1021 site of the PDGFR; S, order parameter; S_{axis}, order parameter of the bond connecting a methyl carbon and its adjacent carbon; $\langle S^2_{axis}\rangle$, averages of the S^2_{axis} values for each methyl type; SH2, Src-homology-2; T_1, spin−lattice relaxation time; $T_{1\rho}$, relaxation time of spin-locked magnetization; 2D, two dimensional.

surface area, number of van der Waals contacts, crystallographic temperature factors, or solvation parameters (Clackson & Wells, 1995).

SH2 domains are modules of approximately 100 residues that bind to proteins containing phosphotyrosine (pTyr) residues and have additional binding specificity depending on the nature of the adjacent amino acids, predominantly those residues C-terminal to the pTyr (Songyang et al., 1993). The C-terminal SH2 domain of the phosphoinositol-specific phospholipase C-γ1 (PLCC SH2) binds with a K_d of ~100 nM (Piccione et al., 1993) to the pY1021 peptide, a 12-residue pTyr containing peptide from its Tyr-1021 binding target on the β-platelet-derived growth factor receptor (PDGFR) (Valius et al., 1993; Valius & Kazlauskas, 1993). The solution NMR structure of the PLCC SH2 domain in complex with the pY1021 peptide has been determined, based primarily on nuclear Overhauser effect (NOE) data (Pascal et al., 1994). The PLCC SH2 domain interacts with eight residues of the pY1021 peptide, from the residue N-terminal to pTyr extending to the amino acid six residues C-terminal to the pTyr (−1 to +6 positions). Over 130 NOEs are observed between the PLCC SH2 domain and peptide residues from the pTyr through Asp +6, leading to a well-determined peptide-binding interface. This extended peptide/protein recognition has also been observed for the N-terminal SH2 domain of the Syp phosphatase (Lee, C. H., et al., 1994) and is distinct from the "two-pronged plug" mode of recognition of the pTyr and the +3 residue demonstrated for the Src (Waksman et al., 1993) and Lck (Eck et al., 1993) SH2 domains.

The dynamics of side chains in the PLCC SH2 domain, both in the free state and in complex with pY1021, have been examined using a novel ^{2}H-based NMR relaxation approach for studying picosecond−nanosecond (ps−ns) time scale dynamics of methyl-containing side chains (Muhandiram et al., 1995). We demonstrate that the PLCC SH2 domain displays restriction of motion in the pTyr binding region, the site which is responsible for a large portion of the binding energy. In contrast, the hydrophobic binding site responsible for recognition of sequences C-terminal to the pTyr displays significant ps−ns motional disorder. These results suggest a correlation between the motional properties of various groups in the PLCC SH2 complex and their importance for high affinity binding and provide insight into the balance between specificity and lack of selectivity in protein recognition.
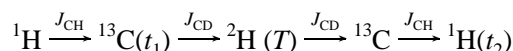
EXPERIMENTAL PROCEDURES

Sample Preparation. The C-terminal SH2 domain used in the present study was expressed from a construct containing residues 663−759 of bovine phosphoinositol-specific phospholipase C-γ1 (Stahl et al., 1988), with an additional three residues at the C-terminus. In order to be consistent with the numbering scheme employed in a previous report (Pascal et al., 1994), the first residue of the construct is numbered Ala-5. The bacteria were grown in M9 minimal media, 65% D$_2$O/35% H$_2$O with ^{15}NH$_4$Cl and [^{13}C$_6$]glucose as the sole nitrogen and carbon sources. Constant time ^{1}H−^{13}C HSQC experiments (Santoro & King, 1992; Vuister & Bax, 1992) which select for either ^{13}CH$_2$D methyl groups or (^{13}CH$_3$ + ^{13}CHD$_2$) methyls were employed to evaluate the deuteration levels of the methyls. The fractional

incorporation of deuterium in the methyls does not reflect the ratio of D$_2$O/H$_2$O used in the growth media, indicating that incorporation is not uniform. In the case of Val, Leu, Ala, and Ile-γ methyls, [CH$_2$D] ~ [CHD$_2$] ~ 2−3×[CH$_3$], while for Thr and Ile-δ, [CH$_2$D] ~ 0.8×[CHD$_2$] ~ 4×[CH$_3$]. In the case of Met, [CH$_2$D] ~ 1.5×[CHD$_2$] ~ 1.2×[CH$_3$]. These results suggest that higher [CH$_2$D] (see below) can be achieved using a 50% D$_2$O/50% H$_2$O ratio in the growth media.

Purification of the triply labeled PLCC SH2 sample was as described previously (Pascal et al., 1994). NMR experiments were performed on a 1.5 mM sample, pH 6.4, 90% H$_2$O/10% D$_2$O, and 0.1 M sodium phosphate, at 30 °C. The pY1021 peptide was synthesized by Dr. Gerald Gish in the lab of Dr. Tony Pawson and contains 12 residues having the sequence Asp-Asn-Asp-pTyr-Ile-Ile-Pro-Leu-Pro-Asp-Pro-Lys. The sample of the peptide complex contained an equimolar ratio of PLCC SH2:pY1021.

NMR Relaxation. The pulse schemes for measuring ^{2}H T_1 and $T_{1\rho}$ relaxation times are given in another publication (Muhandiram et al., 1995) and will therefore only briefly be described here. The magnetization transfer pathway for both T_1 and $T_{1\rho}$ measurements is given by

$$^1\text{H} \xrightarrow{J_{\text{CH}}} {}^{13}\text{C}(t_1) \xrightarrow{J_{\text{CD}}} {}^2\text{H}\,(T) \xrightarrow{J_{\text{CD}}} {}^{13}\text{C} \xrightarrow{J_{\text{CH}}} {}^1\text{H}(t_2)$$

where the active couplings involved in each transfer step are indicated above the arrows and t_1 and t_2 denote the acquisition times. Note that because of both poor deuterium chemical shift dispersion and rapid decay of deuterium magnetization, it is best not to record the ^{2}H chemical shift directly. Hence, relaxation times are obtained in an indirect manner from a series of two-dimensional (^{13}C,^{1}H) constant time spectra. Initially, magnetization is transferred from ^{1}H to ^{13}C via an INEPT transfer (Morris & Freeman, 1979), and subsequently ^{13}C chemical shift is recorded in a constant time manner. During this period, magnetization from methyl groups of the form ^{13}CH$_2$D is selected. During the final $1/(4J_{\text{CD}})$ of the constant time carbon evolution period, where J_{CD} is the one-bond ^{13}C−^{2}H coupling constant, evolution due to this coupling is allowed to occur, facilitating magnetization transfer from ^{13}C to ^{2}H. During the period T, the magnetization is of the form I$_z$C$_z$D$_z$ or I$_z$C$_z$D$_y$ in the T_1 and $T_{1\rho}$ experiments, respectively, where I$_z$, C$_z$, and D$_z$ denote the z magnetization components of the methyl proton, carbon, and deuteron spins, respectively, and D$_y$ is the y component of deuterium magnetization. Therefore, what is actually measured in either the T_1 or the $T_{1\rho}$ experiments is the decay of the triple spin terms, rather than the relaxation of pure deuterium magnetization. Because the decay of the triple spin terms, I$_z$C$_z$D$_z$ and I$_z$C$_z$D$_y$, is dominated by deuterium relaxation, the following relations are an excellent approximation:

$$1/T_1(\text{I}_z\text{C}_z\text{D}_z) = 1/T_1(\text{I}_z\text{C}_z) + 1/T_1(\text{D})$$

$$1/T_{1\rho}(\text{I}_z\text{C}_z\text{D}_y) = 1/T_1(\text{I}_z\text{C}_z) + 1/T_{1\rho}(\text{D}) \qquad (1)$$

where $1/T_1(\text{X})$ is the longitudinal relaxation rate of X. The values of $1/T_1(\text{I}_z\text{C}_z)$ can easily be measured (Muhandiram et al., 1995), and, therefore, $1/T_1(\text{D})$ and $1/T_{1\rho}(\text{D})$ can be obtained in a straightforward manner. After the relaxation period, T, the magnetization is returned to the ^{1}H spin for
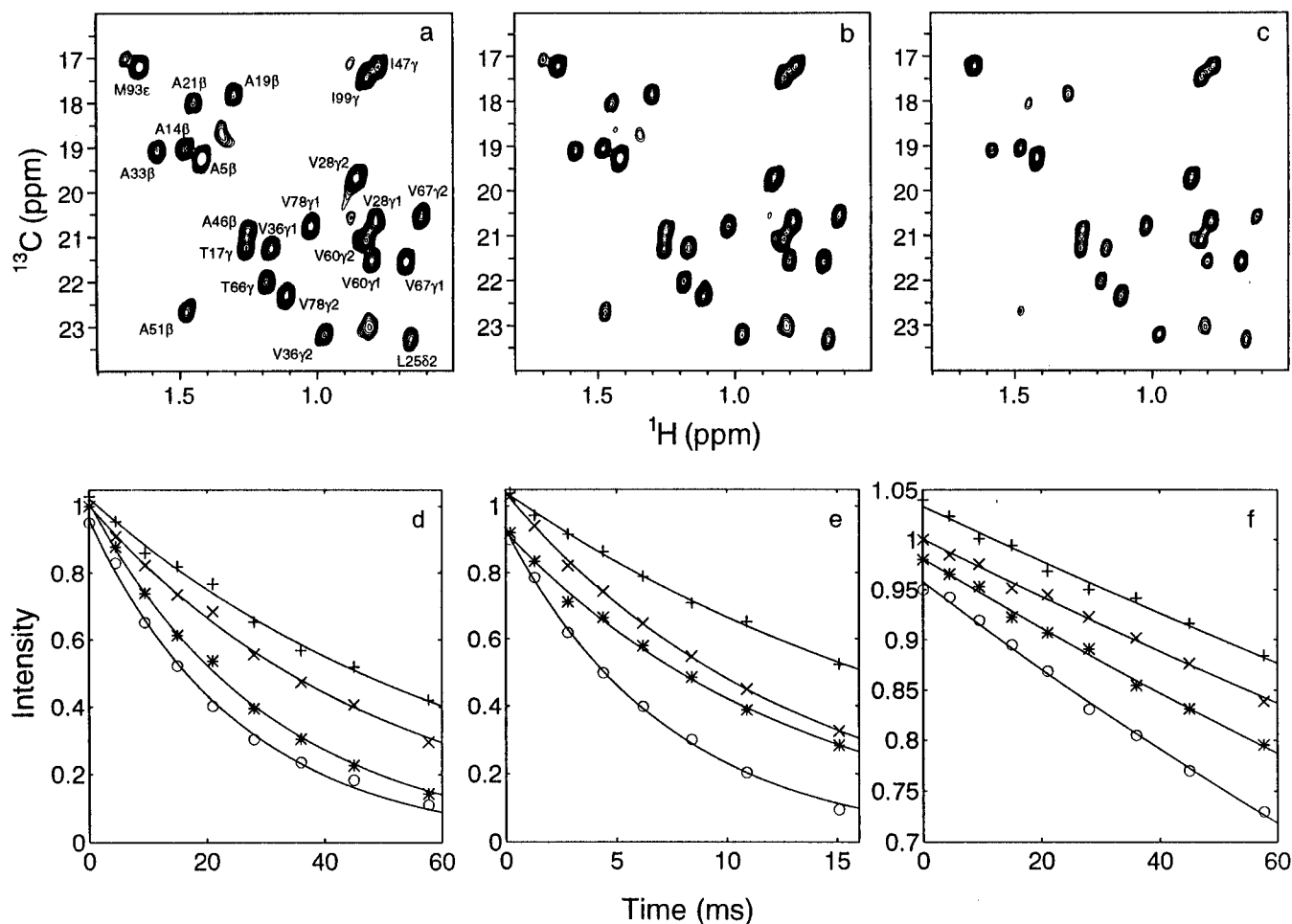
FIGURE 1: Portions of constant-time $^{13}C-^{1}H$ correlation spectra used to measure the decay rates of $I_zC_zD_z$ magnetization of methyls in the free PLCC SH2 domain. Spectra with T values of 50 μs (a), 21 ms (b), and 45 ms (c) are illustrated. Examples of the decay of $I_zC_zD_z$ (d), $I_zC_zD_y$ (e), and I_zC_z (f) magnetization for Met-93 (+), Val-28 γ2 (×), Thr-66 (*) and Ala-51 (○) are also shown. For ease of visualization, a number of the decay curves have been offset.

detection by reversing the transfer steps described above. A more detailed description of the magnetization transfer steps involved in each experiment, the relaxation properties of the triple spin terms, $I_zC_zD_z$ and $I_zC_zD_y$, and justification for measuring deuterium relaxation properties in CH_2D vs CHD_2 methyl groups are given elsewhere (Muhandiram et al., 1995). The effects of cross-correlation between the mechanisms that contribute to the relaxation of $I_zC_zD_z$ and $I_zC_zD_y$ as well as the effects of cross relaxation between all spins within the methyl group and between methyl protons and neighboring protons have been evaluated (Yang & Kay, 1996), and the accuracy of eq 1 has been established for proteins with molecular weights currently amenable for study by NMR.

In order to obtain $T_1(I_zC_zD_z)$ values, nine two-dimensional (2D) spectra were recorded with delays of T = 0.05, 4.5, 9.5, 15, 21, 28, 36, 45, and 57.7 ms. Values of $T_1(I_zC_z)$ were obtained using identical T delays. Values of $T_{1\rho}(I_zC_zD_y)$ were based on eight 2D spectra recorded with delays of T = 0.20, 1.3, 2.8, 4.4, 6.2, 8.4, 10.9, and 15.1 ms. All data sets were recorded as 76 × 576 complex matrices with quadrature obtained in t_1 using States-TPPI (Marion et al., 1989). Spectra were processed and analyzed using routines in nmrPipe (Delaglio, 1993). Spectra were recorded at both 500 and 600 MHz on four-channel UNITY+ spectrometers equipped with actively shielded triple-resonance pulsed field gradient probes. The ^2H lock receiver was disabled during

the periods of deuterium decoupling in the pulse schemes.

The rotational correlation times of the free and complexed states of the PLCC SH2 domain were estimated on the basis of ^{15}N T_1 and T_2 experiments as well as steady-state $^1H-$ ^{15}N NOE experiments, performed on the same sample used to measure deuterium relaxation times. The pulse schemes and the methodology employed are described in detail in Farrow et al. (1994). A value of 7.7 ns was obtained for the free SH2 domain and 6.5 ns for the complexed state. While the free SH2 domain has a tendency to dimerize at the concentrations employed in NMR studies, the extent of dimerization with the construct employed in the present study (see above) is considerably less than previously observed (Farrow et al., 1994) when a slightly different construct, with four additional residues at the amino terminus, was employed. (Note that a correlation time of 9.2 ns was obtained for the free SH2 domain in that study.)

Data Analysis. $T_1(I_zC_zD_z)$, $T_{1\rho}(I_zC_zD_y)$, and $T_1(I_zC_z)$ values were extracted by fitting cross peak intensities to a function of the form

$$I(T) = I(0) \exp(-T/T_i) \qquad (2)$$

where $1/T_i$ ($i=1,1\rho$) is the relevant relaxation rate and $I(T)$ is the intensity of a given cross peak at time T. Errors in measured relaxation rates were estimated using Monte Carlo procedures discussed elsewhere (Farrow et al., 1994). Values

of $T_1(I_zC_zD_z)$, $T_{1\rho}(I_zC_zD_y)$, and $T_1(I_zC_z)$ are provided as Supporting Information. $T_1(D)$ and $T_{1\rho}(D)$ values were extracted from measured values of $T_1(I_zC_zD_z)$, $T_{1\rho}(I_zC_zD_y)$, and $T_1(I_zC_z)$ using eq 1. The measured ^2H relaxation times are related to motional properties at specific sites in the protein through the dependence of T_1 and $T_{1\rho}$ on the power spectral density function, $J(\omega)$, according to the relations (Abragam, 1961):

$$1/T_1 = (3/16)(e^2qQ/\hbar)^2[J(\omega_D) + 4J(2\omega_D)] \quad (3)$$

$$1/T_{1\rho} = (1/32)(e^2qQ/\hbar)^2[9J(0) + 15J(\omega_D) + 6J(2\omega_D)] \quad (4)$$

where e^2qQ/h is the quadrupole coupling constant [165 kHz for methyl deuterons (Burnett & Muller, 1971)]. $J(\omega)$ can be expressed as (Lipari & Szabo, 1982a,b)

$$J(\omega) = (2/5)[S_i^2\tau_m/(1 + (\omega\tau_m)^2) + (1 - S_i^2)\tau_i/(1 + (\omega\tau_i)^2)] \quad (5)$$

where S_i is an order parameter for methyl group i, describing the spatial restriction of motion of the $^{13}C-^2H$ methyl vector on the ns−ps time scale, τ_m is the overall correlation time, and $\tau_i^{-1} = \tau_m^{-1} + \tau_{e,i}^{-1}$ with $\tau_{e,i}$ the effective correlation time describing the internal motions for $^{13}C-^2H$ bond vector i. The order parameter of the bond vector about which the methyl group rapidly rotates (i.e., the bond connecting the methyl carbon and its adjacent carbon) is denoted S_{axis} and is related to S_i by $S_i^2 = 0.111S_{axis}^2$, assuming tetrahedral geometry for the methyl group (Nicholson et al., 1992). More complex forms for $J(\omega)$ can, of course, be assumed, but the values of S_{axis} obtained show little dependence on the model employed (Nicholson et al., 1992). Note that a value of 1 for S_{axis} indicates complete restriction of motion of the methyl averaging axis, while $S_{axis} = 0$ corresponds to complete freedom of motion. Finally, motional parameters were extracted by minimizing the function

$$\chi^2 = \sum[(T_1^c - T_1^e)^2/\sigma_{T_1}^2 + (T_{1\rho}^c - T_{1\rho}^e)^2/\sigma_{T_{1\rho}}^2] \quad (6)$$

where the superscripts c and e refer to calculated and experimentally determined relaxation parameters, respectively, $\sigma_{T_j\,(j\,=\,1,1\rho)}$ is the estimate of the standard deviation of the experimentally determined parameter, T_j, and the summation is over data obtained at both 500 and 600 MHz.

Measurement of Long Range Scalar Coupling Constants. Three bond scalar coupling constants, $^3J_{C\gamma\text{-CO}}$ and $^3J_{C\gamma\text{-N}}$ for Thr, Ile, and Val residues, and $^3J_{C\delta\text{-C}\alpha}$ for Leu and Ile residues were measured to establish the extent of averaging about χ^1 or χ^2 torsion angles. Pulse schemes and methodology developed by Bax and co-workers (Bax et al., 1994) were employed. The PLCC SH2 domain in the samples used for these experiments was uniformly $^{15}N-^{13}C$-labeled (i.e., not fractionally deuterated). Samples of both the short construct and the construct containing four additional N-terminal residues were utilized to provide information for resonances overlapping in spectra of one construct but not the other. Sample conditions were otherwise identical to those given above.

RESULTS

Deuterium T_1 and $T_{1\rho}$ values were determined for methyl deuterons of the isolated PLCC SH2 domain and the PLCC
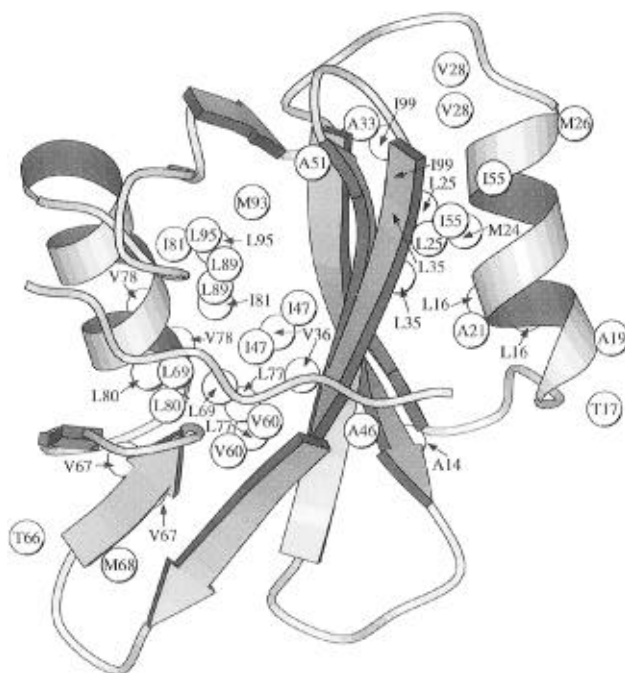

FIGURE 2: Backbone ribbon diagram (Kraulis, 1991) of the solution structure of the PLCC SH2−pY1021 complex with the locations of the methyl groups indicated.

SH2−pY1021 complex at both 500 and 600 MHz. Figure 1 illustrates portions of 2D constant time $^1H-^{13}C$ correlation spectra of the isolated PLCC SH2 domain used to measure the decay of $I_zC_zD_z$ magnetization. Examples of the decay curves for $I_zC_zD_z$, $I_zC_zD_y$, and I_zC_z magnetization of Met-93 ϵ, Val-28 $\gamma2$, Thr-66 γ, and Ala-51 β methyls are also illustrated. The positions of the methyl groups within the PLCC SH2 domain are indicated over the ribbon diagram of the NMR-derived structure (Figure 2). Values of S_{axis}^2 were extracted for 45 of the 47 methyl groups in the free PLCC SH2 domain (Leu-16 $\delta2$ and Leu-25 $\delta1$ cross peaks overlap completely in the free SH2 domain). In the case of the PLCC SH2−pY1021 complex, S_{axis}^2 values for 43 of the 47 methyl groups were determined; resonances of Ile-47 γ and Ile-99 γ and those of Leu-16 $\delta2$ and Leu-25 $\delta1$ completely overlap, preventing their characterization. The values of S_{axis}^2, shown in Figure 3a,b and listed in Table 2 of the Supporting Information, range from approximately 0.1 to 0.95, demonstrating a large range of dynamic behavior for side chain methyl groups. The large distribution of order parameters reported here is quite distinct from measured S^2 values of backbone ^{15}N or $^{13}C\alpha$ atoms, which typically are much less variable, ranging from 0.75 to 0.95 for most nonterminal residues (Kay et al., 1989; Palmer et al., 1991).

The Met methyls, located four atoms away from the backbone, all have S_{axis}^2 values of 0.3 or less. In contrast, Ala methyls, probes of backbone motion, generally display S_{axis}^2 values of 0.8 or higher, with the exception of Ala-5 which is located at the disordered N-terminus. Methyl groups from other residues have S_{axis}^2 values that are, for the most part, between the values measured for Ala and Met residues. In order to correct for this positional dependence, averages of the S_{axis}^2 values for each methyl type, $\langle S_{axis}^2 \rangle$ (Ala C^β, Thr C^γ, Val C^γ, Ile C^γ, Ile C^δ, Leu C^δ, and Met C^ϵ), were calculated, and the difference between S_{axis}^2 and the appropriate $\langle S_{axis}^2 \rangle$ was analyzed. The results are presented in Figure 3c,d. Thus, the S_{axis}^2 values in the
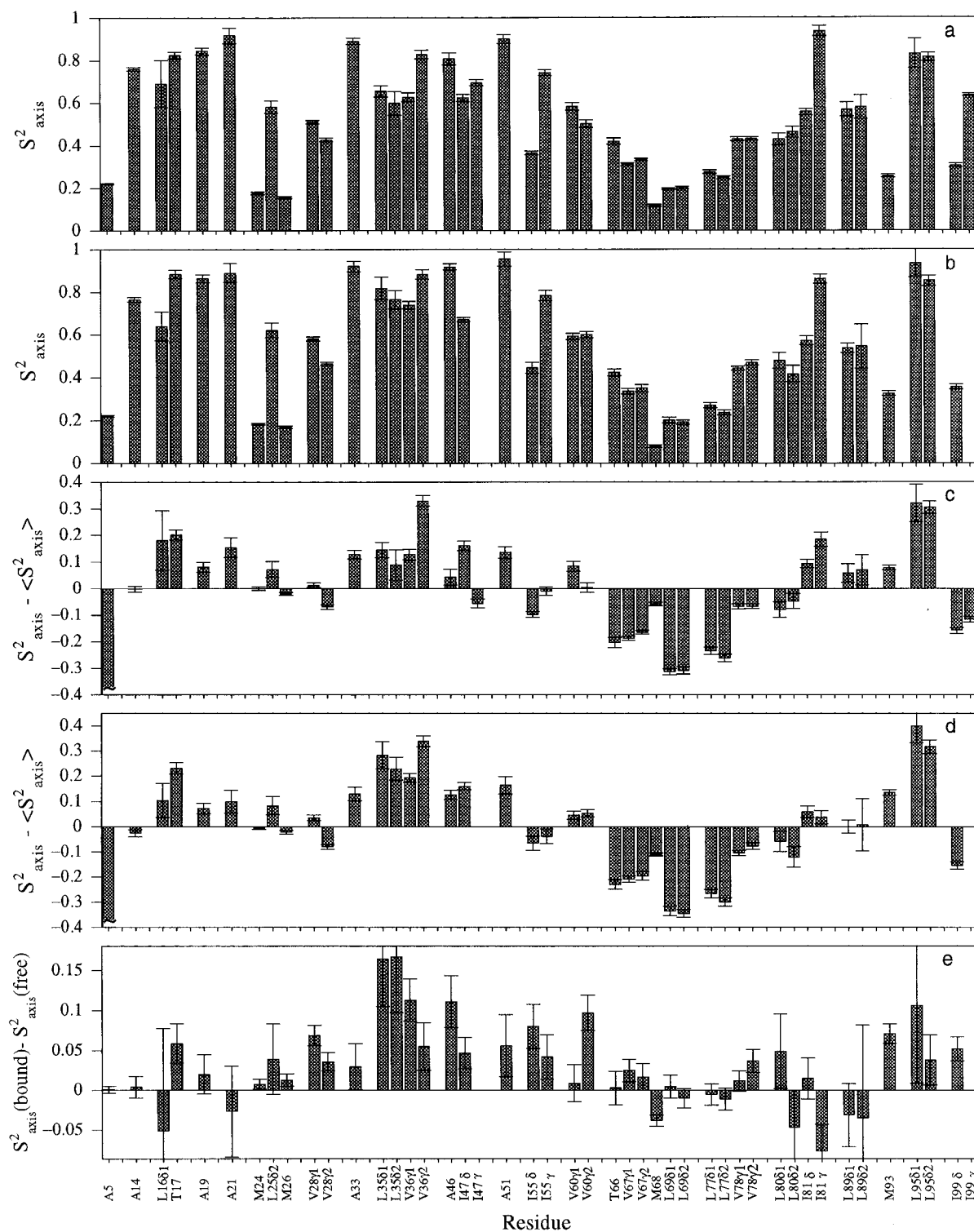
FIGURE 3: Order parameters squared, S^2_{axis}, describing the amplitudes of the motions of the methyl averaging axis (i.e., the bond connecting the methyl carbon and its adjacent carbon) for methyl groups in (a) the free PLCC SH2 domain and (b) the PLCC SH2–pY1021 complex. Differences in S^2_{axis} from the average of the square of order parameters for each methyl type, $\langle S^2_{axis} \rangle$, for methyls of (c) the free PLCC SH2 domain and (d) the PLCC SH2–pY1021 complex. (e) Differences between S^2_{axis} values of methyls in the pY1021-complexed and free states of the PLCC SH2 domain. Error bars are indicated for each value.

N-terminal part of the SH2 domain, particularly in the regions of the pTyr binding site (Leu-35, Val-36, Ala-46) for both the free and complexed states, are higher than average, while some S^2_{axis} values in the hydrophobic binding site (Leu-69, Leu-77) and in the small β-sheet region (Thr-66, Val-67) are significantly lower than average. Note the extremely low values for Leu-69 and Leu-77 methyls. The differences in S^2_{axis} values of the free SH2 and the pY1021-complexed domain (Figure 3e) also show that the pTyr-binding region

is more rigid in the presence of peptide, but that residues in the hydrophobic binding region, responsible for interacting with peptide residues C-terminal to the pTyr, are not significantly affected by peptide binding.

Additional information regarding side chain dynamics is available from measurements of long range homonuclear and heteronuclear scalar coupling constants connecting methyl carbons to carbon or nitrogen nuclei three bonds removed (Bax et al., 1994). Values of $^3J_{C\gamma\text{-CO}}$ and $^3J_{C\gamma\text{-N}}$ for Thr, Ile,

Table 1: Three-Bond Coupling Constants (in Hz) Involving Methyls in the Free and pY1021-Complexed PLCC SH2 Domain[a]

(A)	free		complexed	
	$^3J_{C\gamma\text{-}CO}$	$^3J_{C\gamma\text{-}N}$	$^3J_{C\gamma\text{-}CO}$	$^3J_{C\gamma\text{-}N}$
V28γ1	0.83 (0.11)	1.75 (0.04)	1.06 (0.16)	1.82 (0.03)
V28γ2	3.11 (0.03)	0.57 (0.10)	3.06 (0.05)	<0.5
V36γ1	<1	1.84 (0.08)	<1	1.84 (0.05)
V36γ2	3.63 (0.06)	<0.5	3.68 (0.12)	<0.5
V60γ1	1.10 (0.12)	1.73 (0.06)	<1	1.66 (0.04)
V60γ2	3.36 (0.04)	0.56 (0.18)	3.56 (0.07)	0.55 (0.15)
V67γ1	2.71 (0.03)	0.57 (0.09)	2.82 (0.10)	0.84 (0.04)
V67γ2	1.73 (0.05)	0.69 (0.09)	1.86 (0.15)	0.53 (0.07)
V78γ1	1.48 (0.05)	1.59 (0.03)	1.62 (0.07)	1.61 (0.02)
V78γ2	3.13 (0.03)	<0.5	3.09 (0.04)	<0.5
T17γ	2.97 (0.06)	0.87 (0.14)	2.84 (0.10)	0.76 (0.08)
T66γ	1.67 (0.06)	1.08 (0.06)	1.67 (0.09)	0.93 (0.04)
I47γ	<1	1.87 (0.08)	b	b
I55γ	<1	1.95 (0.07)	<1	2.05 (0.06)
I81γ	<1	2.09 (0.09)	<1	2.11 (0.07)
I99γ	<1	1.70 (0.06)	b	b

(B)	free	complexed
	$^3J_{C\delta\text{-}C\alpha}$	$^3J_{C\delta\text{-}C\alpha}$
L16δ1	c	c
L16δ2	c	c
L25δ1	3.30 (0.06)[d]	e
L25δ2	<1	<1
L35δ1	<1	<1
L35δ2	4.03 (0.10)	3.47 (0.07)
L69δ1	2.46 (0.01)	2.37 (0.02)
L69δ2	2.57 (0.01)	2.98 (0.15)
L77δ1	2.38 (0.01)	2.45 (0.04)
L77δ2	2.46 (0.01)	2.83 (0.02)
L80δ1	3.66 (0.05)	3.44 (0.10)
L80δ2	<1	1.16 (0.13)
L89δ1	1.06 (0.06)	<1
L89δ2	3.94 (0.10)	3.98 (0.18)
L95δ1	4.20 (0.10)	4.35 (0.40)
L95δ2	1.21 (0.12)	1.12 (0.15)
I47δ	3.39 (0.02)	3.26 (0.03)
I55δ	2.84 (0.02)	2.61 (0.07)
I81δ	1.90 (0.06)	1.81 (0.11)
I99δ	2.42 (0.02)	2.16 (0.04)

[a] Errors are given in parentheses. [b] Quantitation difficult due to overlap between I47γ and I99γ resonances. [c] Measured value unreliable due to strong coupling between the Cδ and Cγ resonances. [d] Quantitation suspect due to partial overlap with the L16δ2 resonance. Note that in spectra of the free PLCC SH2 domain (short construct), L16δ2 and L25δ1 overlap completely. In spectra of the free domain with the construct having four extra residues at the N-terminal end (see Experimental Procedures), the overlap is much less severe. The value reported for L25δ1 was measured on this latter construct. [e] Quantitation difficult due to complete overlap with the L16δ2 resonance.

and Val and values of $^3J_{C\delta\text{-}C\alpha}$ for Leu and Ile measured for the isolated PLCC SH2 domain and the pY1021 complex are shown in Table 1. These *J*-coupling constants define χ^1 or χ^2 torsion angles via Karplus type relations (Karplus, 1959, 1963). The magnitude of the couplings can be used to establish which of the three sterically favored staggered rotamer positions are populated. If there is free rotation or significant rotational averaging of the involved torsion angle, the measured *J*-couplings will reflect this. The values of $^3J_{C\gamma\text{-}CO}$ and $^3J_{C\gamma\text{-}N}$ for Thr-66 in both free and complexed states provide evidence of free rotation about χ^1, and those of Val-67 indicate some motion within the $\chi^1 = -60°$ well. The values of $^3J_{C\alpha\text{-}C\delta}$ for Leu-69, Leu-77, and Ile-99 clearly reflect averaging due to free rotation about χ^2 in both free and complexed states and somewhat less so for Ile-81. Note that residues Leu-69, Leu-77, and Ile-81 are located within the hydrophobic binding interface. The couplings measured

Table 2: Recognition Sites for the PLCC SH2 Domain in the PDGFR and Other Proteins Known To Be or To Potentially Be PLCC SH2 Binding Targets[a]

Known sites		Sequence
PDGFR-β	Y1021	GDND<u>YII</u>PLPDPK
EGFR	Y992	DADE<u>YLI</u>PQQGFF
PDGFR-α	Y1018	ADSG<u>YII</u>PDPDID

Potential sites		Sequence
PLCγ1	Y783	NPGF<u>YVEA</u>NPMPT
Flg	Y558	DGPL<u>YVIV</u>EYASK
Erb-B2	Y1120	ETDG<u>YVAP</u>LTCS

[a] The residue number of the pTyr is given, and the pTyr and residues at the +1, +2, and +3 positions are underlined. PDGFR-β (Valius et al., 1993; Valius & Kazlauskas, 1993); epidermal growth factor receptor (EGFR) (Rotin et al., 1992; Ullrich et al., 1984); PDGFR-α (Claesson-Welsh et al., 1989; Eriksson et al., 1995); PLCγ1 (Meisenhelder et al., 1989; G. Gish, personal communication); Flg (Partanen et al., 1991); Erb-B2 (Semba et al., 1985).

for other residues, including those surrounding the pTyr binding region, indicate that single rotamer positions are populated. These results are consistent with the dynamic behavior observed in the ^{2}H-relaxation studies.

DISCUSSION

In principle, NMR relaxation provides a powerful approach for studying protein side chain dynamics, and a number of investigations of methyl dynamics at specific ^{13}C labeled sites in proteins have appeared (Henry et al., 1986; Nicholson et al., 1992). In practice, the interpretation of data from such experiments has been fraught with difficulties due to interference effects between the three ^{13}C−^{1}H dipoles which contribute to the relaxation of the carbon spin (Kay & Torchia, 1991; Werbelow & Grant, 1977). These problems are eliminated with the recently developed methods for measuring ^{2}H relaxation rates in uniformly ^{13}C and fractionally ^{2}H-labeled proteins (Muhandiram et al., 1995). Moreover, this new approach permits measurement of relaxation parameters at each resolved methyl in the protein. This has allowed a comparative study of the dynamics of methyl-containing side chains in both the free and the pY1021-complexed states of the PLCC SH2 domain.

Table 2 shows the recognition site for the PLCC SH2 domain on the PDGFR as well as other known and potential PLCC SH2 binding targets. The sequence similarity among most of these targets in the three residues C-terminal to the pTyr is reasonably strong, with a preference for branched hydrophobic residues in the +1 and +2 positions and Pro in the +3 position. The residues N-terminal to the pTyr tend to be acidic. However, there is considerable divergence of sequence in residues at the +4, +5, and +6 positions, residues shown to interact with the PLCC SH2 domain in the PLCC SH2−pY1021 complex (Pascal et al., 1994). Binding studies by Cantley and co-workers with peptide libraries having randomized sequences at the +1, +2, and

+3 sites reported that the PLCC SH2 domain shows lower selectivity for these three residues than the SH2 domains of Fyn, Crk, Nck, and the C-terminal SH2 domain of the p85 subunit of phosphoinositol-3′-kinase (Songyang et al., 1993). Importantly, studies of truncated peptides derived from the pY1021 peptide have also shown reasonable binding affinity (lowered ∼15-fold) when only the Asp −1, pTyr and Ile +1 residues are present (Wolf et al., 1996). Thus, the pTyr and its immediately adjacent residues are responsible for a major portion of the free energy of binding in this SH2 complex.

The apparent conflict between structural data and the binding results raises a number of interesting questions. First, why do the extensive contacts between the SH2 domain and peptide residues at the +2 through +6 positions not confer significant binding energy or specificity? Second, why are a multiplicity of residues at positions +2 through +6 permissible for binding, and why does reasonable binding occur when these sites are unoccupied? In the case of the Ca^{+2}-binding protein calmodulin which interacts with multiple targets, a group of flexible hydrophobic Met residues on the surface mediates protein interactions (Siivari et al., 1996). Since Met is a long, unbranched, and flexible residue (Lee, K. H., et al., 1994), it is ideally suited to this task. The +2 to +6 binding groove on the PLCC SH2 domain, however, has no Met residues. Instead, there are a number of branched residues (Leu and Val) as well as aromatic (Tyr) and other hydrophobic residues which are normally considered to be conformationally restricted due to steric interactions. Therefore, these data regarding ns−ps motion and torsional averaging in the peptide-binding region are of great interest.

Results demonstrating the extremely low order parameters and averaging of couplings for Leu-69, however, are surprising given that this residue is intimately involved in SH2 domain−peptide contacts, with 14 NOEs to the peptide. Approximately 30% of the 29 observed NOEs to the Pro +3 peptide position, as well as NOEs to the +1, +2, and +5 positions, are provided by Leu-69. In addition, Leu-69 is completely buried in the pY1021 complex, with no surface area accessible to solvent. The values of S^2_{axis} for the two Leu-69 C^δ-methyls are about 0.2. These values are lower than the S^2_{axis} value for the Ala-5 C^β-methyl, which is at the disordered N-terminus of the protein. Crystal structures of peptides (Bendetti, 1977) and proteins (*J*anin et al., 1978) suggest that Leu side chains exist predominantly in only two of the nine possible rotamer conformations ($\chi^1 = -60°$, $\chi^2 = 180°$; $\chi^1 = 180•$, $\chi^2 = 60°$). Solid-state ^{2}H NMR studies indicate that these two side chain conformations interconvert rapidly in both collagen (Batchelder et al., 1982) and in the fd coat protein (Colnago et al., 1987). Such rapid interconversion cannot completely account for the low values of S^2_{axis} measured for either Leu-69 or Leu-77 since a minimum value of 0.33 is predicted from such interconversions (Nicholson et al., 1992). Therefore, Leu-69 and -77 methyls must be experiencing additional motion in order to account for the low values of S^2_{axis}.

The flexibility in the hydrophobic binding surface of the PLCC SH2 domain provides a framework for understanding the relaxed specificity of this domain for target phosphotyrosine-containing sequences. Despite the predominance of branched side chain residues, as opposed to Met residues, the SH2 domain nevertheless presents a highly flexible hydrophobic binding surface similar to that of calmodulin. The region is flexible in the presence and absence of peptide, with no significant increase in S^2_{axis} upon binding. This may be important for minimizing the entropic penalty associated with formation of the peptide−protein complex. This situation is in contrast to the pTyr binding region, where the methyl groups are less mobile and the S^2_{axis} values increase slightly upon binding peptide. The flexibility in the hydrophobic binding surface may also help to explain the minimal free energy imparted by the extensive protein contacts to positions +2 through +6 of the peptide. The combination of significant amplitude motions and the steep distance dependence of the van der Waals potential may well result in a substantial decrease in the interaction energy that would otherwise manifest in a static interaction.

It is interesting to compare these results to those of a previous study of the dynamics of the PLCC SH2−pY1021 complex where broadening of aliphatic resonances of the four Arg residues in the pTyr-binding region was observed, providing evidence of modulation of their chemical shifts by millisecond to microsecond time scale motion (Pascal et al., 1995). Broadening is not observed in any region of the binding interface other than the pTyr-binding site. The modulation may be the result of exchange between various Arg−pTyr interactions due to the large number of hydrogen bonding configurations possible with four Arg residues present. Regions which are rigid on the nanosecond−picosecond time scale probed by NMR relaxation, therefore, show mobility on a millisecond−microsecond time scale, indicating that there need not be a correspondence between different motional regimes. In a similar vein, a lack of correlation between NMR relaxation (ps−ns motion) and hydrogen exchange data (∼millisecond motion) has been noted (Kordel et al., 1992).

It is noteworthy that a number of the residues which display above average amplitudes of motion (i.e., negative values of $S^2_{axis} - \langle S^2_{axis} \rangle$, Figure 3c,d) have very low or zero surface accessibilities in the PLCC SH2−pY1021 complex, including Val-67, Leu-69, and Leu-77. This implies that total burial of surface area does not necessarily guarantee rigid packing and specific interactions, although in the case of significant flexibility, local breathing or cavities must be present. In this regard, the present resolution of NMR structures that have been obtained provide some indication that a buried cavity is located near the hydrophobic binding interface in the PLCC SH2−pY1021 complex.

Despite the relaxed peptide binding specificity of the PLCC SH2 domain, the protein does not indiscriminately bind to any pTyr-containing sequence. The binding studies of Cantley and co-workers demonstrate reasonably strong preferences for branched hydrophobic side chains in the +1 and +2 positions and Pro in the +3 position (Songyang et al., 1993). There is also some selectivity at the +4 and +5 positions, and substitution of Ser for Leu at the +4 position or Lys for Pro at the +5 position reduces binding affinity (Larose et al., 1995). The limited specificity may, in part, be due to Leu-89 which, like Leu-69, contacts the peptide at multiple sites but interacts particularly strongly with the Pro +3 position of the pY1021 peptide. S^2_{axis} values for this residue indicate that it is significantly less flexible than Leu-69. Thus, the balance between rigidity and flexibility in this binding surface may provide a compromise between complete specificity and lack of selectivity in the interactions

of this SH2 domain.

In a recent study by Matthews and co-workers, flexibility was also correlated with plasticity in binding of various ligands to an internal cavity in lysozyme (Morton et al., 1995). It was shown that the binding properties of a variety of ligands could be explained by knowledge of the intrinsic dynamics of the binding site; precise geometry and interaction energies were not required. Thus, establishing the flexibility of binding sites rather than pursuing laborious structural analysis of multiple protein complexes may be sufficient to determine which regions of a protein interface are most important for providing high affinity binding and specificity. Results of ^{2}H relaxation studies similar to those presented here on proteins involved in recognition, such as other SH2 domain−phosphopeptide and ligand−receptor complexes, should be useful in providing an understanding of the factors which lead to the stabilization of specific biological complexes.

ACKNOWLEDGMENT

SUPPORTING INFORMATION AVAILABLE

Tables listing T_1(D), $T_{1\rho}$(D), and $T_1(I_zC_z)$ values at 500 and 600 MHz for both the free PLCC SH2 domain and the pY1021 complex and values of S^2_{axis} and τ_e (6 pages). Ordering information is given on any current masthead page.

REFERENCES

Abragam, A. (1961) *Principles of Nuclear Magnetism*, p 289, Clarendon Press, Oxford.

Batchelder, L. S., Sullivan, C. E., Jelinski, L. W., & Torchia, D. A. (1982) *Proc. Natl. Acad. Sci. U.S.A. 79*, 386.

Bax, A., Vuister, G. W., Grzesiek, S., Delaglio, F., Wang, A. C., Tschudin, R., & Zhu, G. (1994) *Methods Enzymol. 239*, 79.

Bendetti, C. (1977) in *Proceedings of the Fifth American Peptide Symposium* (Goodman, M., & Meienhofer, J., Eds.) p 257, Wiley, New York.

Burnett, L. H., & Muller, B. H. (1971) *J. Chem. Phys. 55*, 5829.

Clackson, T., & Wells, J. A. (1995) *Science 267*, 383.

Claesson-Welsh, L., Eriksson, A., Westermark, B., & Heldin, C.-H. (1989) *Proc. Natl. Acad. Sci. U.S.A. 86*, 4917.

Colnago, L. A., Valentine, K. G., & Opella, S. J. (1987) *Biochemistry 26*, 847.

Delaglio, F. (1993) *NMRPipe System of Software*, National Institutes of Health, Bethesda, MD.

Eck, M. J., Shoelson, S. E., & Harrison, S. C. (1993) *Nature 362*, 87.

Eriksson, A., Nanberg, E., Ronnstrand, L., Engstrom, U., Hellman, U., Rupp, E., Carpenter, G., Heldin, C. H., & Claesson-Welsh, L. (1995) *J. Biol. Chem. 270*, 7773.

Farrow, N. A., Muhandiram, R., Singer, A. U., Pascal, S. M., Kay, C. M., Gish, G., Shoelson, S. E., Pawson, T., Forman-Kay, J. D., & Kay, L. E. (1994) *Biochemistry 33*, 5984.

Henry, G. D., Weiner, J. H., & Sykes, B. D. (1986) *Biochemistry 25*, 590.

Janin, J., Wodak, S., Levitt, M., & Maigret, B. (1978) *J. Mol. Biol. 125*, 357.

Karplus, M. (1959) *J. Chem. Phys. 30*, 11.

Karplus, M. (1963) *J. Am. Chem. Soc. 85*, 2870.

Kay, L. E., & Torchia, D. A. (1991) *J. Magn. Reson. 95*, 536.

Kay, L. E., Torchia, D. A., & Bax, A. (1989) *Biochemistry 28*, 8972.

Klee, C. B., & Vanaman, T. C. (1982) *Adv. Protein Chem. 35*, 213.

Kordel, J., Skelton, N. J., Akke, M., Palmer, A. G., & Chazin, W. J. (1992) *Biochemistry 31*, 4856.

Kraulis, P. J. (1991) *J. Appl. Crystallogr. 24*, 946.

Larose, L., Gish, G., & Pawson, T. (1995) *J. Biol. Chem. 270*, 3858.

Lee, C. H., Kominos, D., Jacques, S., Margolis, B., Schlessinger, J., Shoelson, S. E., & Kuriyan, J. (1994) *Structure 2*, 423.

Lee, K. H., Xie, D., Freire, E., & Amzel, M. A. (1994) *Proteins: Struct., Funct., & Genet. 20*, 68.

Lipari, G., & Szabo, A. (1982a) *J. Am. Chem. Soc. 104*, 4559.

Lipari, G., & Szabo, A. (1982b) *J. Am. Chem. Soc. 104*, 4546.

Marion, D., Ikura, M., Tschudin, R., & Bax, A. (1989) *J. Magn. Reson. 85*, 393.

McCubbin, W. D., & Kay, C. M. (1980) *Acc. Chem. Res. 13*, 185.

Meisenhelder, J., Suh, P. G., Rhee, S. G., & Hunter, T. (1989) *Cell 57*, 1109.

Morris, G. A., & Freeman, R. (1979) *J. Am. Chem. Soc. 101*, 760.

Morton, A., Baase, W. A., & Matthews, B. W. (1995) *Biochemistry 34*, 8564.

Muhandiram, D. R., Yamazaki, T., Sykes, B. D., & Kay, L. E. (1995) *J. Am. Chem. Soc. 117*, 11536.

Nicholson, L. K., Kay, L. E., Baldisseri, D. M., Arango, J., Young, P. E., Bax, A., & Torchia, D. A. (1992) *Biochemistry 31*, 5253.

Palmer, A. G., Rance, M., & Wright, P. E. (1991) *J. Am. Chem. Soc. 113*, 4371.

Partanen, J., Makela, T. P., Eerola, E., Korhonen, J., Hirvonen, H., Claesson-Welsh, L., & Alitalo, K. (1991) *EMBO J. 10*, 1347.

Pascal, S. M., Singer, A. U., Gish, G., Yamazaki, T., Shoelson, S. E., Pawson, T., Kay, L. E., & Forman-Kay, J. D. (1994) *Cell 77*, 461.

Pascal, S. M., Yamazaki, T., Singer, A. U., Kay, L. E., & Forman-Kay, J. D. (1995) *Biochemistry 34*, 11353.

Pawson, T. (1995) *Nature 373*, 573.

Pawson, T., & Schlessinger, J. (1993) *Curr. Biol. 3*, 434.

Piccione, E., Case, R. D., Domchek, S. M., Hu, P., Chaudhuri, M., Backer, J. M., Schlessinger, J., & Shoelson, S. E. (1993) *Biochemistry 32*, 3197.

Rotin, D., Margolis, B., Mohammadi, M., Day, R. J., Daum, G., Li, N., Fischer, E. H., Burgess, W. H., Ullrich, A., & Schlessinger, J. (1992) *EMBO J. 11*, 559.

Santoro, J., & King, G. C. (1992) *J. Magn. Reson. 97*, 202.

Semba, K., Kamata, N., Toyoshima, K., & Yamamato, T. (1985) *Proc. Natl. Acad. Sci. U.S.A. 82*, 6497.

Siivari, K., Zhang, M., Palmer, A. G., & Vogel, H. J. (1996) *FEBS Lett.* (in press).

Songyang, Z., Shoelson, S. E., Chaudhuri, M., Gish, G., Pawson, T., Haser, W. G., King, F., Roberts, T., Ratnofsky, S., Lechleider, R. J., Neel, G. G., Birge, R. B., Fajardo, J. E., Chou, M. M., Hanafusa, H., Schaffhausen, B., & Cantley, L. C. (1993) *Cell 72*, 767.

Stahl, M. L., Feren, C. R., Kellehe, K. L., Kriz, R. W., & Knopf, J. L. (1988) *Nature 332*, 269.

Ullrich, A., Coussens, L., Hayflick, J. S., Dull, T. J., Gray, A., Tam, A. W., Lee, J., Yarden, Y., Libermann, T. A., Schlessinger, J., Downward, J., Mayes, E. L. V., Whittle, N., & Waterfield, M. D. (1984) *Nature 309*, 418.

Valius, M., & Kazlauskas, A. (1993) *Cell 73*, 321.

Valius, M., Bazenet, C., & Kazlauskas, A. (1993) *Mol. Cell. Biol. 13*, 133.

Vogel, H. J. (1994) *Biochem. Cell. Biol. 72*, 357.

Vuister, G. W., & Bax, A. (1992) *J. Magn. Reson. 101*, 201.

Waksman, G., Shoelson, S. E., Pant, N., Cowburn, D., & Kuriyan, J. (1993) *Cell 72*, 779.

Werbelow, L. G., & Grant, D. M. (1977) *Adv. Magn. Reson. 9*, 189.

Wolf, G., Lynch, A., Chaudhuri, M., Gish, G., Pawson, T., & Shoelson, S. E. (1996) *J. Biol. Chem.* (manuscript submitted).

Yang, D., & Kay, L. E. (1996) *J. Magn. Reson.* (in press).